ASEAN Journal of Chemical Engineering 2025, Vol. 25, No. 2, 225 – 240

Radiolytic Degradation of Reactive Orange-16: Degradation Pathways and Kinetics

Fifi Nurfiana [*,1,3]
Rochmadi Rochmadi [1]
Rochim Bakti Cahyono [1]
Hendig Winarno [2]
Jonas Kristanto [1]
Sugili Putra [3]
Waringin M. Yusmaman [3]
Dori Fitria [4]
Dewi Agustiningsih [5]

[1] *Department of Chemical Engineering, Faculty of Engineering, Universitas Gadjah Mada, Jl. Grafika No. 2, Kampus UGM, Yogyakarta 55281, Indonesia*

[2] *Research Center for Radiation Process Technology, National Research and Innovation Agency KST B.J. Habibie, Jl. Puspiptek, Tangerang Selatan, Banten 15314, Indonesia*

[3] *Polytechnic Institute of Nuclear Technology, National Research and Innovation Agency Jl. Babarsari Kotak POB 6101/YKKB, Yogyakarta 55281, Indonesia*

[4] *Chemistry Study Program, Faculty of Science and Technology, UIN Sulthan Thaha Saifuddin, Muaro Jambi, Jambi 36361, Indonesia*

[5] *Department of Chemistry, Faculty of Mathematics and Natural Sciences, Universitas Gadjah Mada, Sekip Utara Bulaksumur, Yogyakarta 55281, Indonesia*

*e-mail: fifi004@brin.go.id

Submitted 16 July 2024 *Revised* 24 June 2025 *Accepted* 19 July 2025

Abstract. Removal of Reactive Orange-16 (RO-16) dye, an emerging water pollutant and potential carcinogen, was investigated using gamma radiation. The radiolytic degradation process was studied in a batch reactor with a gamma-ray dose rate of 2426 Gy/h. Degradation of 96% RO-16 dye was achieved at 3.0 kGy irradiation dose (0.1 mM initial dye concentration). Twelve degradation products were predicted based on the m/z results from liquid chromatography-high resolution mass spectrometry (LC-HRMS). Among these, acetic acid and formic acid were identified. Possible degradation pathways were predicted based on the observed degradation products. The concentrations of the reactants RO-16, acetic acid, and formic acid were quantified to determine a specific kinetic model. The initial breakdown of the molecule occurred slowly, as indicated by the small *k* value, due to the steric hindrance of the large RO-16 molecule. As the molecule became smaller, the *k* value increased, indicating that the molecular breakdown process became faster, ultimately leading to the formation of end products. The formation of smaller molecular mass degradation products indicated that the gamma irradiation process is a promising alternative for the potential degradation of RO-16 dye.

Keywords: Degradation Path, Gamma-Ray, Reactive Orange-16, Specific Kinetics

DOI: 10.22146/ajche.14820

INTRODUCTION

Water pollution is a worldwide issue that poses a threat to the entire ecosystem (Martin *et al*., 2023). Reactive Orange-16 (RO-16) is a type of reactive azo dye, which is the most commonly used. Azo dyes account for an estimated 60-70% of all dyes used (R. Ananthashankar, 2013). These dyes are characterized by –N=N– bonds linked to aromatic groups, known as chromophores, which impart colour and make the dyes resistant to degradation (Atay *et al*., 2019). Although biological processes are cost-effective for treating certain municipal and industrial wastewaters, studies indicate that traditional biological methods are insufficient for effectively breaking down azo dyes and their aromatic components (Punzi *et al*., 2015). RO-16 dye poses environmental risks due to its toxicity and mutagenic properties, and the body can easily absorb it as it is water-soluble (Gunasegaran *et al*., 2020). Therefore, it is crucial to degrade this dye before releasing it into the environment.

Combining biological treatment (bioremediation) with advanced oxidation processes (AOPs) is recognized as an efficient method for degrading azo dyes or decolorizing textile waste (Anouar *et al*., 2014; Martin *et al*., 2023). Various AOP techniques for degrading RO-16 include photodegradation under UV light (Bilgi and Demir, 2005), anodic oxidation with boron-doped diamond electrodes *(Migliorini et al*., 2011), UV/H_2O_2 oxidation (Mitrović *et al*., 2012), photocatalysis with TiO_2 (Kaur *et al*., 2015), and ozonolytic degradation (Muniyasamy *et al*., 2020).

Ionizing radiation, gamma-ray, is a promising AOP for complex mixtures as it can break down bio-recalcitrant species, producing by-products that can be further treated biologically (Madureira *et al*., 2018). Several studies on the degradation of the day using gamma-rays have been conducted, including the degradation of Reactive Blue-19 dye (Arshad *et al*., 2020), Disperse Red-73 dye degradation *(Jamil et al*., 2020), Congo Red dye degradation (Shah *et al*., 2020), Alizarin Yellow GG dye degradation (Sun *et al*., 2013), and Erythrosine dye degradation (Zaouak *et al*., 2019).

In this study, the degradation of RO-16 dye using gamma irradiation was investigated. A key benefit of radiolytic processes is that they do not require the addition of any other chemicals to wastewater, aligning with green chemistry principles.

During the irradiation of water, three reactive intermediates are generated, specifically: hydroxyl radicals ($^{\bullet}OH$), solvated electrons (e_{aq}^{-}), and a hydrogen atom ($H^{\bullet}$), as can be seen in Eq. (1), which can degrade many organic compounds in water (Abdel Rahman & Hung, 2020; Wojnárovits and Takács, 2008). The radiation chemical yield (G-value, μmol·J^{-1}) measures the number of species produced per 100 eV of absorbed energy (Abdel Rahman & Hung, 2020). The yields (G-values) are well-known: in pure water, the yields of $^{\bullet}OH$, e_{aq}^{-}, and $H^{\bullet}$ are 0.28, 0.28, and 0.06 μmol J^{-1}, respectively (Abdel Rahman & Hung, 2020)(Kovács *et al*., 2014). The degradation of the dyes is solely initiated by $^{\bullet}OH$ attacking electron-rich sites on the dye molecules (Rauf & Ashraf, 2009).

$$H_2O \rightarrow {}^{\bullet}OH\ (0.28),\ e_{aq}^{-}\ (0.28),\ {}^{\bullet}H\ (0.06) \qquad (1)$$

It is clarified that the attack by radicals on aromatic rings results in the rings breaking apart and forming carboxylic acids, acetaldehyde, and other degradation products in the solution (Madureira *et al*.,

2020; Wang & Chu, 2016). However, a major challenge with AOPs is the creation of reaction degradation products, which may be resistant or potentially more toxic than the original compounds.

Identifying and characterizing these degradation products is a complex task for researchers in this field. Liquid chromatography-mass spectrometry (LC-MS) is frequently used to identify degradation products in the aqueous phase (Arshad *et al*., 2020; Kalsoom *et al*., 2012; Zhang *et al*., 2015).

In recent years, time-of-flight mass spectrometry (TOF-MS) and hybrid quadrupole TOF (QTOF) MS/MS systems, coupled with ultra-high performance liquid chromatography (UHPLC), have emerged as the preferred techniques for separating, monitoring, and identifying the reaction intermediates generated during water treatment (Frindt *et al*., 2017; Sijumon *et al*., 2017). For organic and inorganic ions, ion chromatography (IC) is utilized *(Shah et al*., 2020).

In this research, the generated degradation products were detected using liquid chromatography-high resolution mass spectrometry (LC-HRMS), and a possible degradation pathway was predicted based on the observed degradation products. High-resolution mass spectrometry (HRMS) provides the benefits of precise mass measurement and detailed fragmentation data, facilitating the accurate characterization and structural identification of compounds (Qi *et al*., 2023). Additionally, HRMS is advantageous for isolating target ions from various potential interferences and other chemical backgrounds in complex samples (Decheng *et al*., 2022).

The objective of this study was to investigate the radiolytic degradation of RO-16 dye using gamma radiation as an advanced oxidation process. Kinetic modeling was employed to enhance understanding of the degradation mechanism and was validated against experimental data. An iterative approach was utilized to estimate each kinetic rate constant (*k*), comparing experimental results with predicted values of adjusted dependent variables. Optimal values for each *k* were determined by minimizing the standard least-squares error, a method successfully employed in various studies with intricate reaction kinetic schemes (Madureira *et al*., 2020). The overarching aim was to develop versatile kinetic models applicable to technologies based on free-radical reactions.

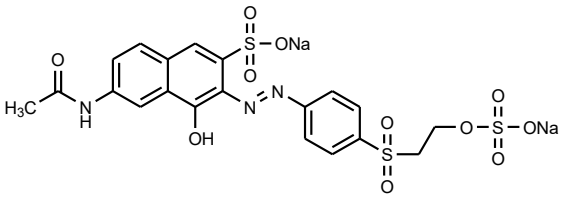

Fig. 1: Molecule structure of RO-16 dye

EXPERIMENTAL SECTION

Materials

Reactive orange-16 (RO-16) with dye content ≥70% was purchased from Sigma Aldrich (Figure 1), water for LCMS (Merck, Germany), acetonitrile (Merck, Germany), acetic acid (Merck, Germany), formic acid (Merck, Germany), and sulfuric acid (Merck, Germany).

Instrumentations

A type I gamma irradiator with a Co-60 radioactive source was used to irradiate the sample. The irradiator was installed at the Polytechnic Institute of Nuclear Technology BRIN with a dose rate of 2426 Gy/h. The RISO

High Dose Reference Laboratory has calibrated the irradiator at the Technical University of Denmark. B3 DoseStix was used as a dosimeter. The Shimadzu 1780 UV-Vis Spectrophotometer was used to analyze the RO-16 concentrations. The Thermo Scientific LC-HRMS was used to identify the degradation product. The Agilent HPLC was used to quantify the degradation products (acetic acid and formic acid).

Sample Irradiation

In each experiment, 250 ml of aqueous dye solution with initial concentrations of 0.1 mM of RO-16 dye was irradiated in a gamma irradiation chamber at certain dose 0, 0.5, 1.0, 1.5, 2.0, 3.0, 4.0, and 5.0 kGy, or at irradiation time 742, 1483, 2226, 2968, 4452, 5936, and 7419 seconds. During irradiation, the solution was rotated at a constant 10 rpm. A 15 ml aliquot was taken to analyze the RO-16 concentration with a UV–Vis spectrophotometer. Dye concentrations were determined from the calibration curve, which was established by relating the concentration to the absorbance measured at 493 nm.

A 100 ml sample was evaporated using a vacuum rotary evaporator at a vacuum pressure of 72 mbar, a bath temperature of 40 °C, and a condenser temperature of 15 °C. This process was carried out until the sample was concentrated to approximately four times its original concentration. The samples resulting from this concentration process will be used for qualitative analysis with the LC-HRMS instrument and quantification of product degradation using the HPLC instrument.

LC-HRMS Analysis

The degradation product analysis utilized liquid chromatography coupled with a hybrid quadrupole-orbitrap high-resolution mass spectrometer. Thermo Scientific Phenyl-Hexyl 100 mm × 2.1 mm ID × 2.6 µm analytical columns were used for liquid chromatography. Mobile phases consisted of MS-grade water (A) and MS-grade acetonitrile (B), using a gradient method with a flow rate of 0.3 mL/min. Initially, mobile phase B was set at 5% and increased gradually to 90% over 16 min. It was then held at 90% for 4 min before returning to the initial condition (5% B) by 25 min. The column temperature was maintained at 40°C, and a 3 µL injection volume was used. The spray voltage was set at 3.30 kV, with a capillary temperature of 320°C and an auxiliary gas heater temperature of 30°C. The scan range was 50–750 m/z in both positive and negative ionization modes.

HPLC Analysis

Analysis of acetic acid and formic acid concentration was performed using Agilent HPLC with a Hi-plex H column (300 mm × 7.7 mm, 8 µm) at 65 °C column temperature. The sample injection volume was 20 µL, and 0.005 N sulfuric acid was used as the mobile phase with a flow rate of 0.5 mL/min. The detector wavelength was 220 nm.

Data Treatment

Kinetic data analysis was conducted using the Python programming language, utilizing Spyder 5.5.5 on a Windows 10 operating system.

RESULTS AND DISCUSSION

The Degradation Pathways of RO-16 Dye by Radiolytic Degradation

The LC–HRMS analysis indicated that the RO-16 dye (MW 617,54 g/mol) was successfully degraded to form smaller

molecules. Ten organic compounds as degradation products (DPs) were detected with the LC-HRMS instrument at certain M/Z mentioned in Table 1. However, not all the products were detected, i.e., sodium 2-(phenylsulfonyl)ethyl sulfate (DP2) and formic acid (DP12). This could be related to the reaction rate constants or the limited sensitivity of the analysis. LC-HRMS cannot detect formic acid because its molecular weight is lower than the m/z scanning range of the instrument. However, when tested with a standard formic acid solution using HPLC, a peak was observed at the same retention time as the standard solution, indicating the presence of formic acid in the sample. Besides that, two inorganic DPs, i.e., H_2SO_4 and H_2O_2, were formed from ˙OH-based degradation of RO-16 dye.

The organic DPs were generated through reactions involving electron transfer, oxidation, and bond cleavage. The possible degradation pathways were predicted based on the observed degradation products. The proposed degradation pathways are shown in Figure 2.

The conversion of RO-16 into DP1, DP2, and DP3 was followed by an attack of ·OH at the C–N single bond between the azo group and the aromatic ring. C-N single bonds cleavage mechanisms were mentioned in several literature (Nemr *et al*., 2018; Özen *et al*., 2004).

The DP1 species further loses the SO_3Na, OH, azo, and acetamide groups to form the DP4, DP5, DP6, and DP7.

Cleavage of the aromatic hydrocarbons of DP2 formed DP8. Bond cleavage and molecular restructuring of DP2 formed DP9 according to Figure 3, and formed DP10 according to Figure 4.

The C-N Bond cleavage on the RO-16 acetamide group formed the acetic acid (DP11). Fragmentation of DP11 formed the formic acid (DP12). Formic acid and acetic acid can also be obtained through the ring opening of aromatic intermediates when compounds of degradation products undergo further degradation (Bansal *et al*., 2010; Mitrović *et al*., 2014; Nemr *et al*., 2018).

Kinetic Modeling of RO-16 Dye Degradation

This study involves determining the rate equation based on the proposed model. The remaining RO-16 reactant, along with degradation products such as acetic acid (DP11) and formic acid (DP12), were quantified to determine the degradation kinetics. Other degradation products are labeled as DP1 to DP10, following the coding in Table 1.

The kinetic model expression is illustrated in Figure 5 and Equations 3-15. The degradation of RO-16 dye by hydroxyl radicals yields intermediate molecules DP1 to DP10, which are further degraded into acetic acid (DP11) and formic acid (DP12). Formic acid will decompose into final products, namely carbon dioxide and water.

The rate of hydroxyl radical formation is determined by the product of the irradiation dose rate (D) and the G-value of ˙OH (Eq. (2)), where D and G are 0.6738 Gy/s and 2.8 x 10^{-7} mol/J, respectively (Rauf and Ashraf, 2009). The irradiation dose rate in Gy/s is converted to J/s. In an aqueous solution with a density of approximately 1 kg/L, 1 Gy/s is equivalent to 1 J/s.

$$R(\cdot OH) = D \times G(\cdot OH) \quad (2)$$

Table 1. RO-16 Dye degradation products identified by HRMS

Code	Compound Name	Structure formula	m/z	Molecular Weight	Status
DP1	Sodium 6-acetamido-3-diazenyl-4-hydroxynaphthalene-2-sulfonate	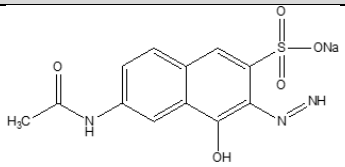	330.04	331.02	Detected
DP2	sodium 2-(phenylsulfonyl)ethyl sulfate	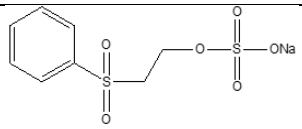	-	287.97	Not detected
DP3	$C_8H_9N_2NaO_6S_2$	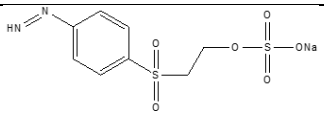	315.21	315.98	Detected
DP4	Sodium 2-diazenyl-3-hydroxybenzenesulfonate	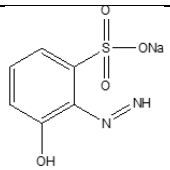	223.05	223.99	Detected
DP5	Sodium 6-acetamido-3-diazenylnaphthalene-2-sulfonate	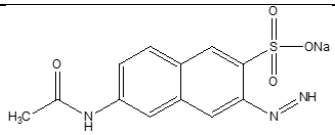	315.21	315.03	Detected
DP6	N-(8-hydroxynaphthalen-2-yl) acetamide	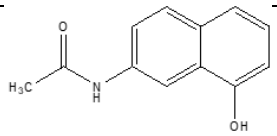	201.05	201.08	Detected
DP7	$C_{12}H_{11}N_3O_2$	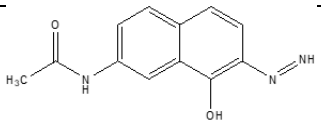	229.04	229.09	Detected
DP8	Sodium (E)-2-(buta-1,3-dienylsulfonyl) ethyl sulfate	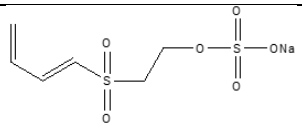	264.05	263.97	Detected
DP9	4-(2-Hydroxyethyl) phenyl hydrogen sulfate	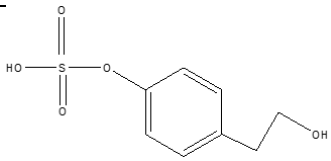	218.03	218.02	Detected
DP10	4-ethyl-2,6-dihydroxyphenyl hydrogen sulfate	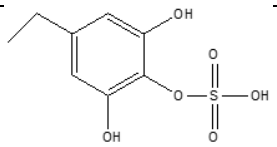	234.03	234.02	Detected
DP11	Acetic acid	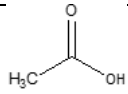	60.04	60.02	Detected
DP12	Formic acid	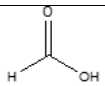	-	46.01	Detected in HPLC

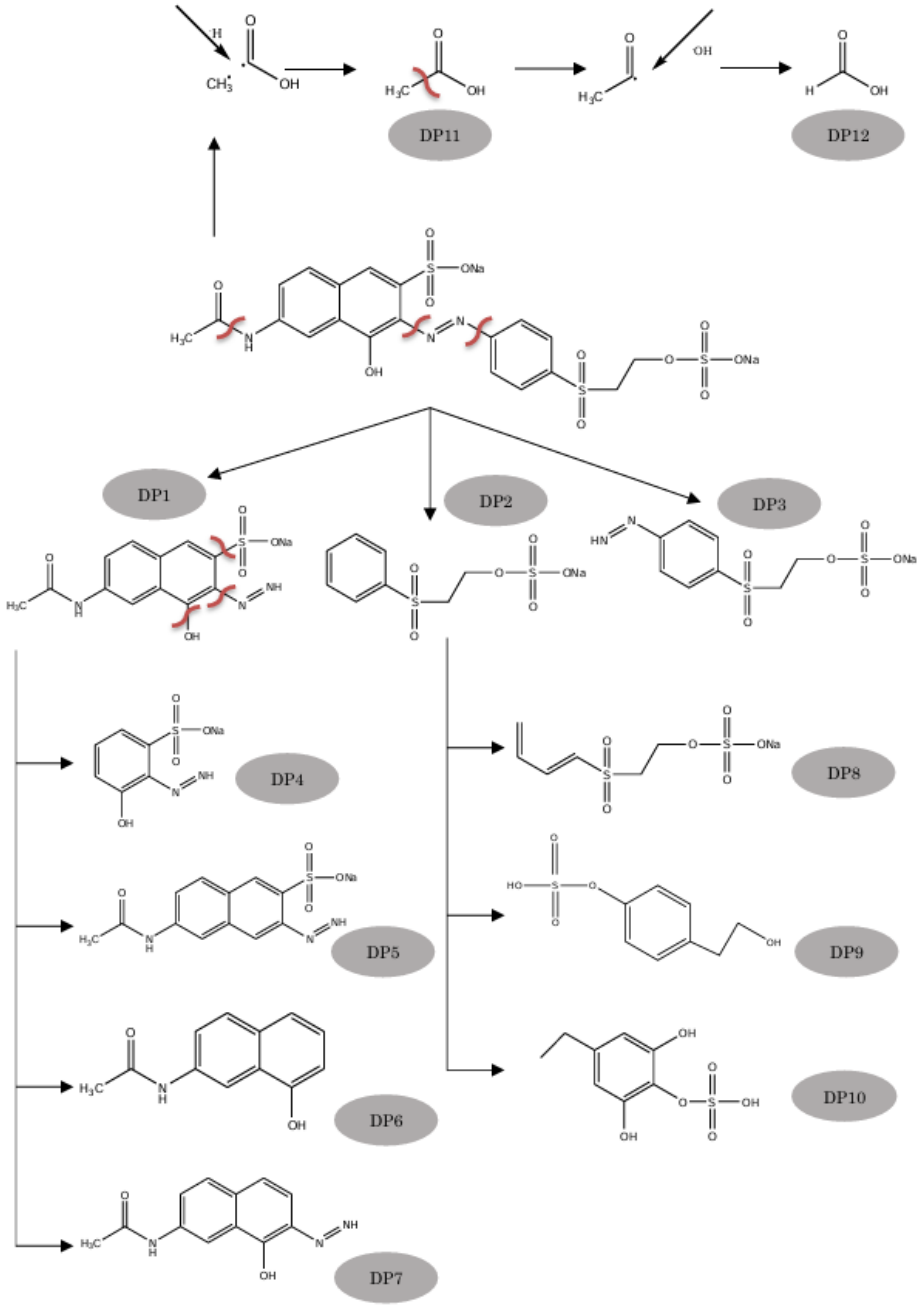

Fig. 2**:** Proposed degradation pathways of RO-16 dye by gamma radiolytic

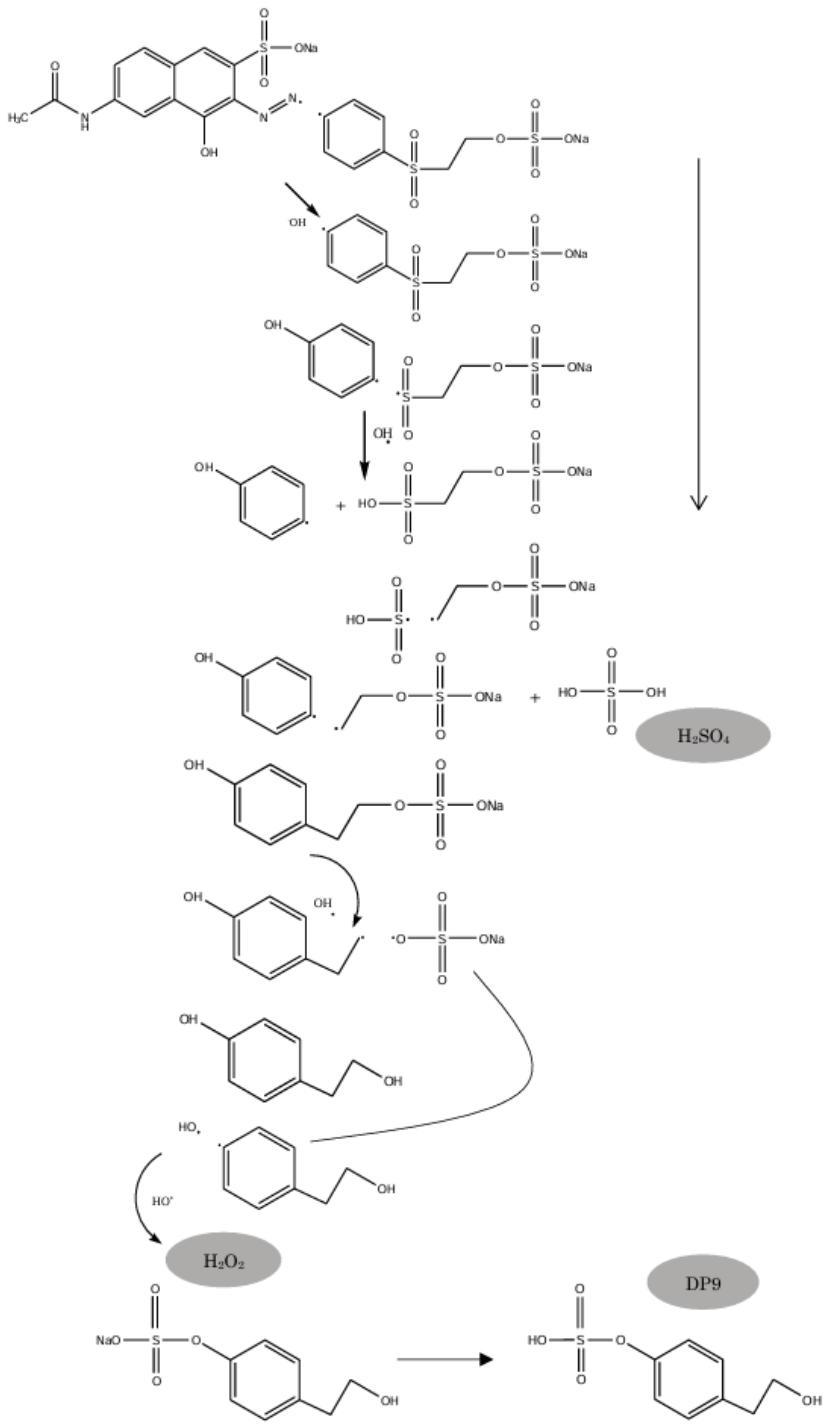

Fig. 3: Bond cleavage and molecular restructuring of RO-16 to form the DP9

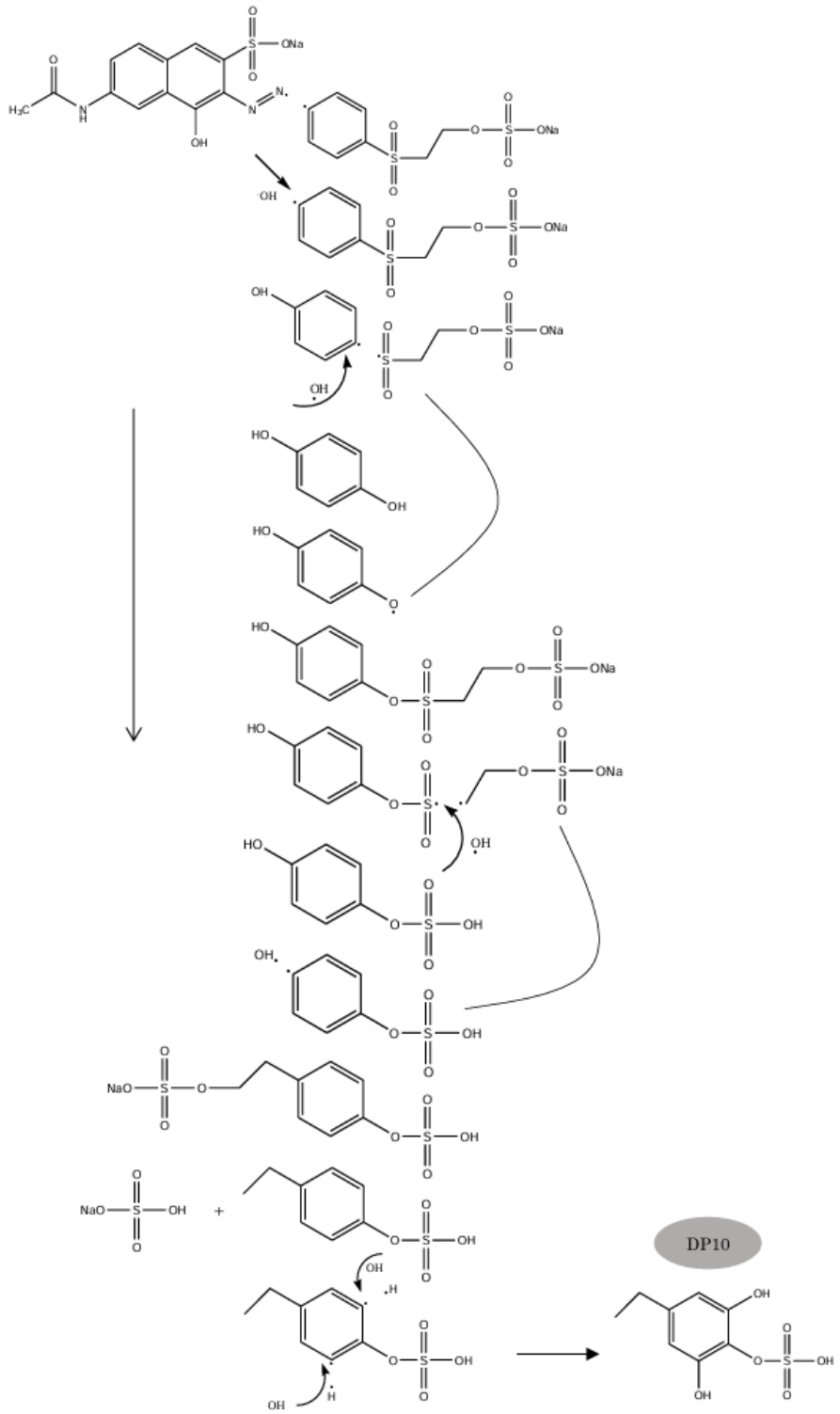

Fig. 4: Bond cleavage and molecular restructuring of RO-16 to form the DP10

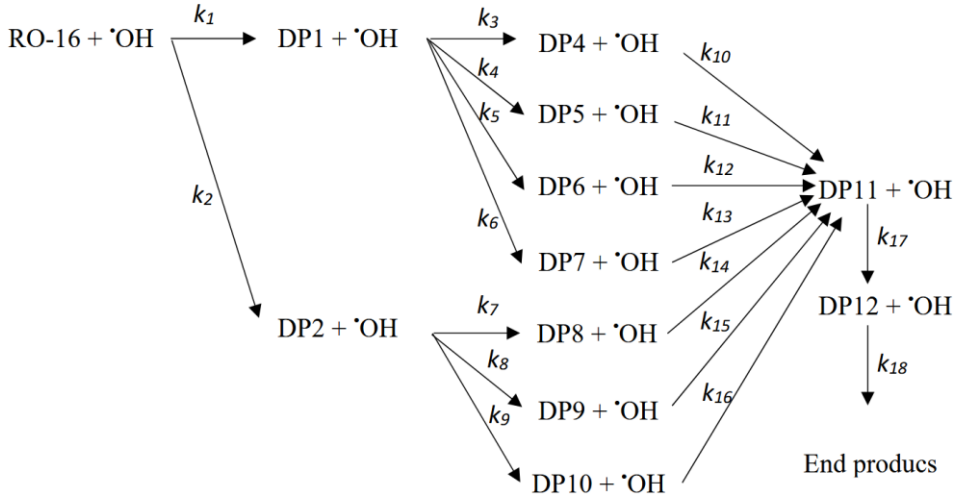

Fig. 5: Specific Kinetics Model for the Degradation of RO-16 Dye

$$\frac{dRO16}{dt} = (-k_1\,[RO16][\cdot OH] - k_2\,[RO16][\cdot OH])V \tag{3}$$

$$\frac{d\cdot OH}{dt} = D \times G(\cdot OH) + (-k_1\,[RO16][\cdot OH] - k_2\,[RO16][\cdot OH] - k_3\,[DP1][\cdot OH] - k_4\,[DP1][\cdot OH] - k_5\,[DP1][\cdot OH] - k_6\,[DP1][\cdot OH] - k_7\,[DP2][\cdot OH] - k_8\,[DP2][\cdot OH] - k_9\,[DP2][\cdot OH] - k_{10}\,[DP4][\cdot OH] - k_{11}\,[DP5][\cdot OH] - k_{12}\,[DP6][\cdot OH] - k_{13}\,[DP7][\cdot OH] - k_{14}\,[DP8][\cdot OH] - k_{15}\,[DP9][\cdot OH] - k_{16}\,[DP10][\cdot OH] - k_{17}\,[DP11][\cdot OH] - k_{18}\,[DP12][\cdot OH])V \tag{4}$$

$$\frac{dDP1}{dt} = (k_1\,[RO16][\cdot OH] - k_3\,[DP1][\cdot OH] - k_4\,[DP1][\cdot OH] - k_5\,[DP1][\cdot OH] - k_6\,[DP1][\cdot OH])V \tag{5}$$

$$\frac{dDP2}{dt} = (k_2\,[RO16][\cdot OH] - k_7\,[DP2][\cdot OH] - k_8\,[DP2][\cdot OH] - k_9\,[DP2][\cdot OH])V \tag{6}$$

$$\frac{dDP4}{dt} = (k_3\,[DP1][\cdot OH] - k_{10}\,[DP4][\cdot OH])V \tag{7}$$

$$\frac{dDP5}{dt} = (k_4\,[DP1][\cdot OH] - k_{11}\,[DP5][\cdot OH])V \tag{8}$$

$$\frac{dDP6}{dt} = (k_5\,[DP1][\cdot OH] - k_{12}\,[DP6][\cdot OH])V \tag{9}$$

$$\frac{dDP7}{dt} = (k_6\,[DP1][\cdot OH] - k_{13}\,[DP7][\cdot OH])V \tag{10}$$

$$\frac{dDP8}{dt} = (k_7\,[DP2][\cdot OH] - k_{14}\,[DP8][\cdot OH])V \tag{11}$$

$$\frac{dDP9}{dt} = (k_8\,[DP2][\cdot OH] - k_{15}\,[DP9][\cdot OH])V \tag{12}$$

$$\frac{dDP10}{dt} = (k_9\,[DP2][\cdot OH] - k_{16}\,[DP10][\cdot OH])V \tag{13}$$

$$\frac{dDP11}{dt} = (3k_{10}\,[DP4][\cdot OH] + 6k_{11}\,[DP5][\cdot OH] + 6k_{12}\,[DP6][\cdot OH] + 6k_{13}\,[DP7][\cdot OH] + 3k_{14}\,[DP8][\cdot OH] + 4k_{15}\,[DP9][\cdot OH] + 4k_{16}\,[DP10][\cdot OH] - k_{17}\,[DP11][\cdot OH])V \tag{14}$$

$$\frac{dDP12}{dt} = (2k_{17}\,[DP11][\cdot OH] - k_{18}\,[DP12][\cdot OH])V \tag{15}$$

The experimental results indicated that the concentration of RO-16 dye decreased rapidly, reaching 96% of its initial concentration at a dose of 3.0 kGy and an irradiation time of 4452 seconds. On the other hand, acetic acid and formic acid, as degradation products, were formed and then disappeared. This reduction was due to the formation of even smaller molecules.

The kinetic constants were evaluated based on the sum of square errors (SSE) of the concentrations of reactive orange-16, acetic acid, and formic acid.

$$SSE = \sum((C_i)_{calculated} - (C_i)_{data})^2 \quad (16)$$

The best-fit specific constants, k_i, in Eqs. (3)–(15) are presented in Table 2. The largest value of k is k_{11}, which is similar to k_{12} and k_{13}. These values represent the degradation of DP5, DP6, and DP7 into DP11 or acetic acid, respectively. These degradation products are structurally similar, containing the aromatic ring derived from the naphthalene moiety of the RO-16 dye, but with differing side chains or branching groups. It is proposed that the naphthalene intermediate is attacked by hydroxyl radicals through a conjugate addition mechanism, resulting in the formation of simple carboxylic acids (Meetani *et al.*, 2011). According to various studies, acetic acid can be readily produced from the ring-opening of aromatic intermediates during further degradation (Bansal *et al.*, 2010; Mitrović *et al.*, 2014; Nemr *et al.*, 2018).

The smallest value of k is found in k_3, which represents the reaction converting DP1 to DP4. DP1 contains two aromatic rings, making it relatively difficult to cleave one of the rings to form DP4. This pathway is less favored due to the existence of alternative reaction routes that are more energetically favorable, resulting in faster reaction rates for those pathways. Specifically, this pertains to the conversion of DP1 into DP5, DP6, and DP7 through the release of its branching groups.

Table 2. Specific Rate Constants for the Radiolytic Degradation of Reactive Orange-16 Dye Solution Based on the Proposed Model

Reaction rate constant	Parameter value (s^{-1})
k_1	0,1971
k_2	3,1 x 10^{-6}
k_3	5,3 x 10^{-7}
k_4	1,0779
k_5	1,0742
k_6	1,0774
k_7	1,7935
k_8	0,9196
k_9	0,9355
k_{10}	0,2457
k_{11}	1,8682
k_{12}	1,8677
k_{13}	1,8652
k_{14}	0,4118
k_{15}	0,3935
k_{16}	0,3930
k_{17}	0,1975
k_{18}	0,2457

$[RO16]_0$= 0.1 mM, D= 2426 Gy/h= 0.6738 Gy/s, G ·OH= 2.8 x 10^{-7} mol/J.

Additionally, k_2, which represents the degradation rate of RO-16 to DP2, also has a low value. This reaction occurs relatively slowly due to the steric hindrance associated with the RO-16 molecule. RO-16 is a large molecule with numerous branches, making it highly susceptible to steric hindrance (Li *et al.*, 2016). The values of k8 and k9 are similar to and lower than those of k7. This is because the degradation products DP2 must undergo multiple restructuring steps to form DP9 and DP10, as illustrated in Figures 3 and 4.

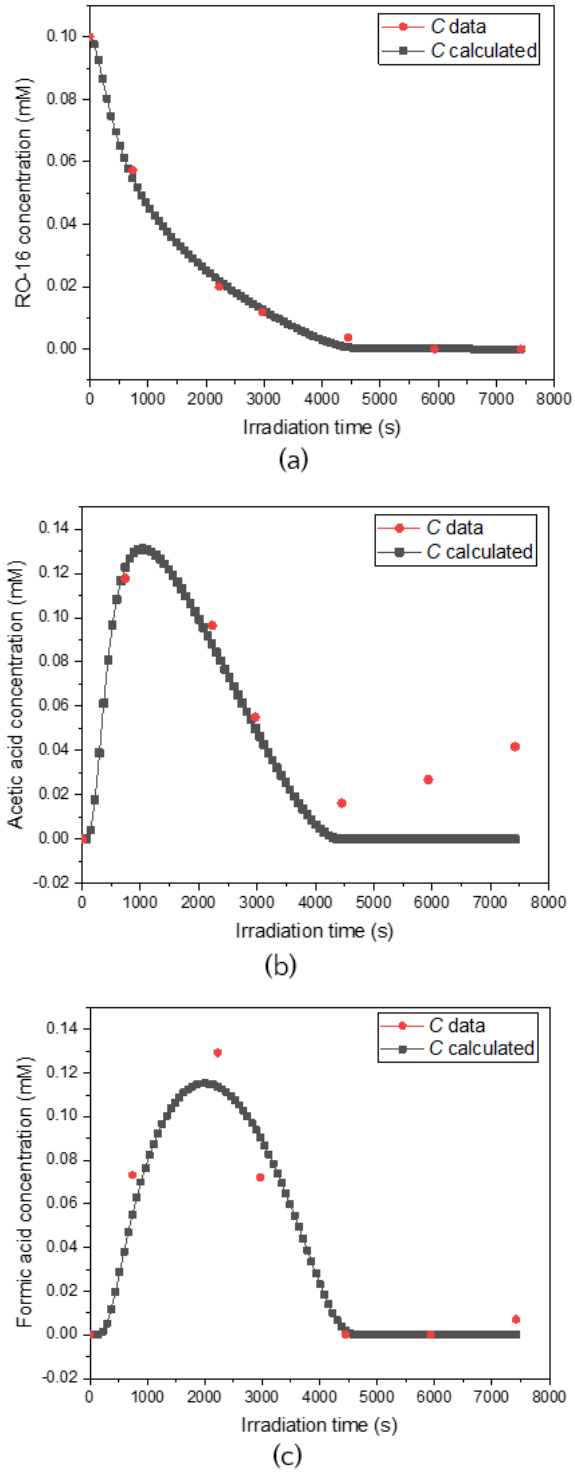

Fig. 6: Comparison of Experimental Concentration Data (C data) and Simulation Model Results (C calculated) for: (a) Reactive Orange-16, (b) acetic acid, (c) formic acid

Figures 6 (a-c) display the experimental data points alongside the model calculation data for reactant and product concentrations. Observed differences between the experimental data and the model may be attributed to several factors, such as simplified assumptions. The developed model relies on simplified assumptions regarding the system under study, including the presumption of uniform radiation distribution, constant reaction rates, G-value data taken from literature, and the exclusion of certain secondary reactions due to the inability to measure other degradation products aside from acetic acid and formic acid. Such simplifications can lead to discrepancies when compared to the more complex realities of the experimental system.

CONCLUSIONS

The findings presented in this manuscript demonstrate the effective application of gamma rays for the degradation of the Reactive Orange-16 dye. The LC-HRMS method is effective for carrying out quantitative analysis. The major radiolytic compounds were identified, and their structures were suggested. Based on this, degradation pathways were proposed, and a kinetic model of the general reaction sequence for degradation was developed. The innovative methodological approach could enhance the understanding of the radiolytic degradation of azo dyes, offering deeper insights into the reaction mechanisms of other resistant compounds.

ACKNOWLEDGEMENT

The authors gratefully acknowledge financial and infrastructure support from the National Research and Innovation Agency for this work.

REFERENCES

Abdel Rahman, R.O., and Hung, Y.T., 2020. "Application of ionizing radiation in wastewater treatment: An overview." *Water 12 (1), 19*. https://doi.org/10.3390/w12010019

Anouar, H., Elhassan, A., Hourch, A. El, and Kacemi, K. El, 2014. "Electronic and optical properties of reactive orange 16 azo dye." *Int. J. Innov. Appl. Stud. 8*, 1447–1454.

Arshad, R., Bokhari, T.H., Khosa, K.K., Bhatti, I.A., Munir, M., Iqbal, Mazhar, Iqbal, D.N., Khan, M.I., Iqbal, Munawar, and Nazir, A., 2020. "Gamma radiation induced degradation of anthraquinone Reactive Blue-19 dye using hydrogen peroxide as oxidizing agent." *Radiat. Phys. Chem. 168*, 108637. https://doi.org/10.1016/j.radphyschem.2019.108637

Atay, Ç.K., Kart, S.Ö., Gökalp, M., Tuğrul, Ö., and Tilki, T., 2019. "Characterization and absorption properties of newly synthesized mono azo dyes: Experimental and theoretical approach." *J. Mol. Struct. 1180*, 251–259. https://doi.org/10.1016/j.molstruc.2018.11.108

Bansal, P., Singh, D., and Sud, D., 2010. "Photocatalytic degradation of azo dye in aqueous TiO_2 suspension: Reaction pathway and identification of intermediates products by LC/MS." *Sep. Purif. Technol. 72*, 357–365. https://doi.org/10.1016/j.seppur.2010.03.005

Bilgi, S., and Demir, C., 2005. "Identification of photooxidation degradation products of C.I. Reactive Orange 16 dye by gas chromatography-mass spectrometry." *Dye. Pigment. 66*, 69–76. https://doi.org/10.1016/j.dyepig.2004.08.007

Decheng, S., Xia, F., Zhiming, X., Liyang, and Peilong, W., 2022. "Simultaneous determination of eight carbapenems in milk by modified QuEChERS and ultra high performance liquid chromatography coupled with high-field quadrupole-orbitrap high-resolution mass spectrometry." *J. Chromatogr. A 1670*, 462979. https://doi.org/10.1016/j.chroma.2022.462979

Frindt, B., Mattusch, J., Reemtsma, T., Griesbeck, A.G., and Rehorek, A., 2017. "Multidimensional monitoring of anaerobic/aerobic azo dye based wastewater treatments by hyphenated UPLC-ICP-MS/ESI-Q-TOF-MS techniques." *Environ. Sci. Pollut. Res. 24*, 10929–10938. https://doi.org/10.1007/s11356-016-7075-5

Gunasegaran, M., Ravi, S., and Shoparwe, N.F., 2020. "Kinetic studies of Reactive Orange 16 (RO16) dye removal from aqueous solution using PIMs." *J. Phys. Conf. Ser. 1529*, 052003. https://doi.org/10.1088/1742-6596/1529/5/052003

Jamil, A., Bokhari, T.H., Iqbal, M., Bhatti, I.A., Zuber, M., Nisar, J., and Masood, N., 2020. "Gamma radiation and hydrogen peroxide based advanced oxidation process for the degradation of disperse dye in aqueous medium." *Zeitschrift fur Phys. Chemie, 234*, 279–294. https://doi.org/10.1515/zpch-2019-1384

Kalsoom, U., Ashraf, S.S., Meetani, M.A., Rauf, M.A., and Bhatti, H.N., 2012. "Degradation and kinetics of H_2O_2 assisted photochemical oxidation of

Remazol Turquoise Blue." *Chem. Eng. J. 200–202*, 373–379. https://doi.org/10.1016/j.cej.2012.06.058

Kaur, N., Shahi, S.K., and Singh, V., 2015. "Anomalous behavior of visible light active TiO_2 for the photocatalytic degradation of different Reactive dyes." *Photochem. Photobiol. Sci. 14*, 2024–2034. https://doi.org/10.1039/c5pp00165j

Kovács, K., Mile, V., Csay, T., Takács, E., and Wojnárovits, L., 2014. "Hydroxyl radical-induced degradation of fenuron in pulse and gamma radiolysis: kinetics and product analysis." *Environ. Sci. Pollut. Res. 21*, 12693–12700. https://doi.org/10.1007/s11356-014-3197-9

Li, R., Song, X., Huang, Y., Fang, Y., Jia, M., and Ma, W., 2016. "Visible-light photocatalytic degradation of azo dyes in water by Ag_3PO_4: An unusual dependency between adsorption and the degradation rate on pH value." *J. Mol. Catal. A Chem. 421*, 57–65. https://doi.org/10.1016/j.molcata.2016.05.009

Madureira, J., Barros, L., Melo, R., Cabo Verde, S., Ferreira, I.C.F.R., and Margaça, F.M.A., 2018. "Degradation of phenolic acids by gamma radiation as model compounds of cork wastewaters." *Chem. Eng. J. 341*, 227–237. https://doi.org/10.1016/j.cej.2018.02.036

Madureira, J., Leal, J.P., Botelho, M.L., Cooper, W.J., and Melo, R., 2020. "Radiolytic degradation mechanism of acetovanillone." *Chem. Eng. J. 382*, 122917. https://doi.org/10.1016/j.cej.2019.122917

Martin, M.M., Sumayao, R.E., Soriano, A.N., and Rubi, R.V.C., 2023. "Photocatalytic degradation activity of the biosynthesized r. rosifolius mediated silver nanoparticles in methylene blue dye." *ASEAN J. Chem. Eng. 23*, 329–342. https://doi.org/10.22146/ajche.82506

Migliorini, F.L., Braga, N.A., Alves, S.A., Lanza, M.R.V., Baldan, M.R., and Ferreira, N.G., 2011. "Anodic oxidation of wastewater containing the Reactive Orange 16 Dye using heavily boron-doped diamond electrodes." *J. Hazard. Mater. 192*, 1683–1689. https://doi.org/10.1016/j.jhazmat.2011.07.007

Mitrović, J., Radović, M., Bojić, D., Anbelković, T., Purenović, M., and Bojić, A., 2012. "Decolorization of the textile azo dye Reactive Orange 16 by the UV/H_2O_2 process." *J. Serbian Chem. Soc. 77*, 465–481. https://doi.org/10.2298/JSC110216187M

Mitrović, J.Z., Radović, M.D., Andelković, T.D., Bojić, D. V., and Bojić, A.L., 2014. "Identification of intermediates and ecotoxicity assessment during the UV/H_2O_2 oxidation of azo dye Reactive Orange 16." *J. Environ. Sci. Heal. - Part A Toxic/Hazardous Subst. Environ. Eng. 49*, 491–502. https://doi.org/10.1080/10934529.2014.859022

Muniyasamy, A., Sivaporul, G., Gopinath, A., Lakshmanan, R., Altaee, A., Achary, A., and Velayudhaperumal Chellam, P., 2020. "Process development for the degradation of textile azo dyes (mono-, di-, poly-) by advanced oxidation process - Ozonation: Experimental & partial derivative modelling approach." *J. Environ. Manage. 265, 110397.*

https://doi.org/10.1016/j.jenvman.2020.110397

Nemr, A. El, Hassaan, M.A., and Madkour, F.F., 2018. "Advanced Oxidation Process (AOP) for detoxification of Acid Red 17 dye solution and degradation mechanism." *Environ. Process.* 5, 95–113. https://doi.org/10.1007/s40710-018-0284-9

Özen, A.S., Aviyente, V., De Proft, F., and Geerlings, P., 2004. "Modeling the substituent effect on the oxidative degradation of azo dyes." *J. Phys. Chem. A,* *108*, 5990–6000. https://doi.org/10.1021/jp037138z

Punzi, M., Anbalagan, A., Aragão Börner, R., Svensson, B.M., Jonstrup, M., and Mattiasson, B., 2015. "Degradation of a textile azo dye using biological treatment followed by photo-Fenton oxidation: Evaluation of toxicity and microbial community structure." *Chem. Eng. J.* *270*, 290–299. https://doi.org/10.1016/j.cej.2015.02.042

Qi, P., Zhou, Q., Chen, G., Lin, Z., Zhao, J., Xu, H., Gao, H., Liu, D., and Mao, X., 2023. "Simultaneous qualitative and quantitative determination of 104 fat-soluble synthetic dyes in foods using disperse solid-phase extraction and UHPLC-Q-Orbitrap HRMS analysis." *Food Chem.* *427*, 136665. https://doi.org/10.1016/j.foodchem.2023.136665

R Ananthashankar, A.G., 2013. "Production, characterization and treatment of textile effluents: A critical review." *J. Chem. Eng. Process Technol.* *05*, 1–18. https://doi.org/10.4172/2157-7048.1000182

Rauf, M.A., and Ashraf, S.S., 2009. "Radiation induced degradation of dyes-An overview." *J. Hazard. Mater.* *166*, 6–16. https://doi.org/10.1016/j.jhazmat.2008.11.043

Shah, N.S., Khan, J.A., Sayed, M., Khan, Z.U.H., Iqbal, J., Arshad, S., Junaid, M., and Khan, H.M., 2020. "Synergistic effects of H_2O_2 and $S_2O_8^{2-}$ in the gamma radiation induced degradation of congo-red dye: Kinetics and toxicities evaluation." *Sep. Purif. Technol.* *233*, 115966. https://doi.org/10.1016/j.seppur.2019.115966

Sijumon, V.A., Aravind, U.K., and Aravindakumar, C.T., 2017. "Degradation of amaranth dye using zero valent iron nanoparticles: optimal conditions and mechanism." *Environ. Eng. Sci.* *34*, 376–383. https://doi.org/10.1089/ees.2016.0340

Sun, W., Chen, L., Tian, J., Wang, J., and He, S., 2013. "Degradation of a monoazo dye Alizarin Yellow GG in aqueous solutions by gamma irradiation: Decolorization and biodegradability enhancement." *Radiat. Phys. Chem.* *83*, 86–89. https://doi.org/10.1016/j.radphyschem.2012.10.014

Wang, J., and Chu, L., 2016. "Irradiation treatment of pharmaceutical and personal care products (PPCPs) in water and wastewater: An overview." *Radiat. Phys. Chem.* *125*, 56–64. https://doi.org/10.1016/j.radphyschem.2016.03.012

Wojnárovits, L., and Takács, E., 2008. "Irradiation treatment of azo dye containing wastewater: An overview." *Radiat. Phys. Chem.* *77*, 225–244. https://doi.org/10.1016/j.radphyschem.2007.05.003

Zaouak, A., Noomen, A., and Jelassi, H., 2019. "Gamma radiolysis of erythrosine dye in aqueous solutions." *J. Radioanal. Nucl.*

Chem. *321*, 965–971. https://doi.org/10.1007/s10967-019-06671-x

Zhang, R., Yuan, D.X., and Liu, B.M., 2015. "Kinetics and products of ozonation of C.I. Reactive Red 195 in a semi-batch reactor." *Chinese Chem. Lett.* *26*, 93–99. https://doi.org/10.1016/j.cclet.2014.10.024